SCIENCE CHINA
Earth Sciences

• RESEARCH PAPER •

November 2011 Vol.54 No.11: 1696–1715
doi: 10.1007/s11430-011-4218-x

Late-Quaternary strong earthquakes on the seismogenic fault of the 1976 M_s7.8 Tangshan earthquake, Hebei, as revealed by drilling and trenching

GUO Hui, JIANG WaLi* & XIE XinSheng

Institute of Crustal Dynamics, China Earthquake Administration, Beijing 100085, China

Received November 9, 2010; accepted February 14, 2011; published online July 23, 2011

Composite borehole profiling combined with trenching is an effective way to acquire evidence of past ruptures of buried active faults. In this study, three composite borehole profiles and a large-scale trench excavation were carried out across the surface rupture zone of the 1976 M_s7.8 Tangshan earthquake. The following three major conclusions have been reached. (1) The surface rupture zone of the 1976 earthquake extends more than 47 km long to the south of Tangshan city, passing to the west of Sunjialou, to Daodi town in Fengnan County, to Xihe in Fengnan County. (2) The surface rupture zone is divided into south and north branches. The north branch has mainly right-lateral strike-slip motion, and the vertical displacement of the surface is up on the west and down on the east. On the other hand, the vertical displacement of the south branch is up on the east and down on the west, accompanied by some right-lateral slip. Such a faulting style cannot be explained by the movement of a single normal or reverse fault, but is consistent with the vertical displacement field induced by the right-lateral strike-slip of the fault belt. The drilling and trenching data from this study verify that such activity continued through the Late Quaternary on the Tangshan Fault. (3) The fault planes exhumed by trenching and the dislocations of strata revealed by the boreholes indicate that multiple faulting events occurred on the Tangshan Fault in the Late Quaternary. The timing of three ruptures prior to the 1976 earthquake was 7.61–8.13, >14.57, and 24.21–26.57 ka BP. Counting the earthquake of 1976, the recurrence interval of the four strong events is about 6.7 to 10.8 ka. On one of the three borehole profiles, the Niumaku profile, nine faulting events were detected since 75.18 ka BP with an average interval of 8.4 ka. In addition, this paper also discusses the difference between the Late Quaternary sedimentary environments to the north and south of Tangshan city based on stratum dating.

Tangshan earthquake, surface rupture zone, multi-stage activity, earthquake recurrence interval, paleoseismic trenching, borehole profile

Citation: Guo H, Jiang W L, Xie X S. Late-Quaternary strong earthquakes on the seismogenic fault of the 1976 M_s7.8 Tangshan earthquake, Hebei, as revealed by drilling and trenching. Sci China Earth Sci, 2011, 54: 1696−1715, doi: 10.1007/s11430-011-4218-x

The M_s7.8 Tangshan earthquake of 1976 in the northern North China Plain was the largest earthquake in the region over the last 300 years and had a death toll of 242 thousand people. In the first nationwide seismic intensity zonation map published in 1957 [1], Tangshan was on the border of an intensity VIII region. However, during the process of seismic fortification undertaken in eastern Hebei Province, focus was placed on the Luanxian area where two historical $M6\frac{1}{4}$ earthquakes had been recorded. In the historic records, the largest earthquake recorded in Tangshan was the $M4\frac{1}{4}$ earthquake of 1935. The M_s7.8 Tangshan earthquake of 1976 produced an intensity of XI that devastated many inadequately fortified buildings in Tangshan. Tangshan city is situated at the southern foot of the Yanshan Mountain, where was the uplift area during Tertiary period. The seis-

*Corresponding author (email: walijianghdc@vip.sina.com)

mogenic structure of the strong near-magnitude-8 earthquake that took place in such a tectonic setting is therefore especially interesting for researchers in China and abroad.

Since the Tangshan earthquake in 1976, research into its seismogenic structure can be divided into two stages. In the first stage, opinions concerning the seismogenic structure were put forward based on both field investigations and observational data before and after the earthquake. These can be summarized as follows. (1) Based on field investigations, a surface rupture zone caused by the earthquake was identified in the south of Tangshan city, which was 8 to 11 km long, trending NE30° with a maximum right-lateral strike slip of 1.5–2.3 m and a vertical displacement of 0.2–0.7 m [2–5]. (2) Ground deformation and seismic data have been used to invert for the seismogenic structure of the Tangshan earthquake [6–12], which is characterized by a rupture striking NE30° to 49°, with a dip of 76°–90°, a rupture length of 84–140 km, a maximum right-lateral strike slip of 1.36–4.59 m, and a vertical displacement of 0.5–0.7 m. (3) As for deep structures in the vicinity of Tangshan, seismic sounding has indicated that there are anomalies in the Moho and upper mantle structure [13], resulting in a 2.5 km down throw of an intracrust interface on the east side [14, 15]. On the seismic reflection profile at a depth of 18–22 km beneath Tangshan, there is a propagation anticline and steep fault on a fault ramp [16]. Additionally, to the south of Tangshan city, transient magnetic prospecting has shown that throws of 200 m and 800 m exist at 2 and 6–8 km below the surface, respectively [17]. (4) Paleoearthquakes, Quaternary fault activities, and seismogenic structures in the Tangshan area have also been reported [18–21]. Based on the liquefaction phenomenon characterized by paleoseismic trench, ^{14}C dating of strata, and the sedimentation rate, Wang and Li [18] inferred that strong earthquakes occurred in the Tangshan area at 7 and 14 ka B.P.

The second stage of the Tangshan earthquake study started in the late 1990s. As the reconstruction of Tangshan city progressed, shallow seismic soundings provided more information on the Tangshan Fault. Such as, the fault had broken a number of Pleistocene-Holocene strata. The northern section of the fault is a reverse fault; the southern section is a normal fault. The stratum at 175–193 m below the surface has been offset by 18 m, and the throw of the stratum 20 m below surface is 2.4 m [22–24]. During this period, a larger scope for the seismogenic fault of Tangshan earthquake has been proposed based on the surface deformation induced by the earthquake [25]; related problems have also been discussed [26]. Although 34 years have now passed since the earthquake, the complexity and hidden nature of the Tangshan earthquake's seismogenic structure is limited to the results of surface rupture investigations and seismic sounding data. There is a lack of convincing geological evidence on the Late Quaternary activity of the Tangshan Fault.

Based on the above, and to advance understanding of the seismogenic structure of Tangshan earthquake, we carried out a field investigation of the surface rupture zone of the Tangshan earthquake, and undertook the development of composite borehole profiles at three sites and trenching at one site. The primary survey data and results are presented below.

1 Geologic structures and surface rupture zone of Tangshan earthquake

1.1 Geologic structural background

Tangshan is situated at the junction of the southern margin of the Yanshan Mountain with the North China Plain. The terrain is high in the north and low in the south. Changshan-Weishan Mountain to the north of Tangshan City is a relatively low feature on the southern margin of the Yanshan Mountain, and constitutes the northern boundary of the alluvial-proluvial plain in southern Tangshan. The Dacheng Mountain and Fenghuang Mountain are relic mountains of basement rock distributed within Tangshan City, and are southwestward extensions of Changshan-Weishan Mountain in the north. The NNE-trending Douhe River originates from the southern margin of the Yanshan Mountain, traverses Tangshan city from north to south, and flows southward into Bohai Bay (Figure 1).

The geological structural setting of Tangshan is a part of the Kailuan sag-fold system of the Yanshan fold belt. The basement structure of the region is the NE-trending Kaiping synclinorium formed in the Yanshan stage, the nucleus of which consists of Paleozoic rocks. In the Early Paleozoic, exceptionally-rich littoral plain type coal-bearing formations were developed in this region, giving rise to the famous Kaiping coal field. Unlike many buried fault-depresssions in the North China Plain that formed from the Late Mesozoic to the Early Cenozoic, Tangshan city was an uplifted area in Mesozoic and Early Cenozoic time. Mesozoic and Tertiary sediments are missing in the area, and the Quaternary system that is tens to a hundred or so meters thick lies directly on the upper Paleozoic system. Tangshan city is located on the western wing of the Kaiping synclinorium, where there are a number of NNE-trending, parallel, and eastward-thrusting faults. On the south side of Tangshan City, the NNE-trending Cangdong Fault is a regional large fault that controls the boundary between the Cangzhou Uplift and Huanghua Depression.

1.2 The surface rupture zone of the Tangshan earthquake

After the M_s7.8 Tangshan earthquake of 1976, the surface rupture zone south of Tangshan City was extensively investigated. Published reports show that Guo et al. [2], Yang [4] and Du et al. [5] had basically the same opinion on the distribution of the surface rupture zone. That is, the rupture

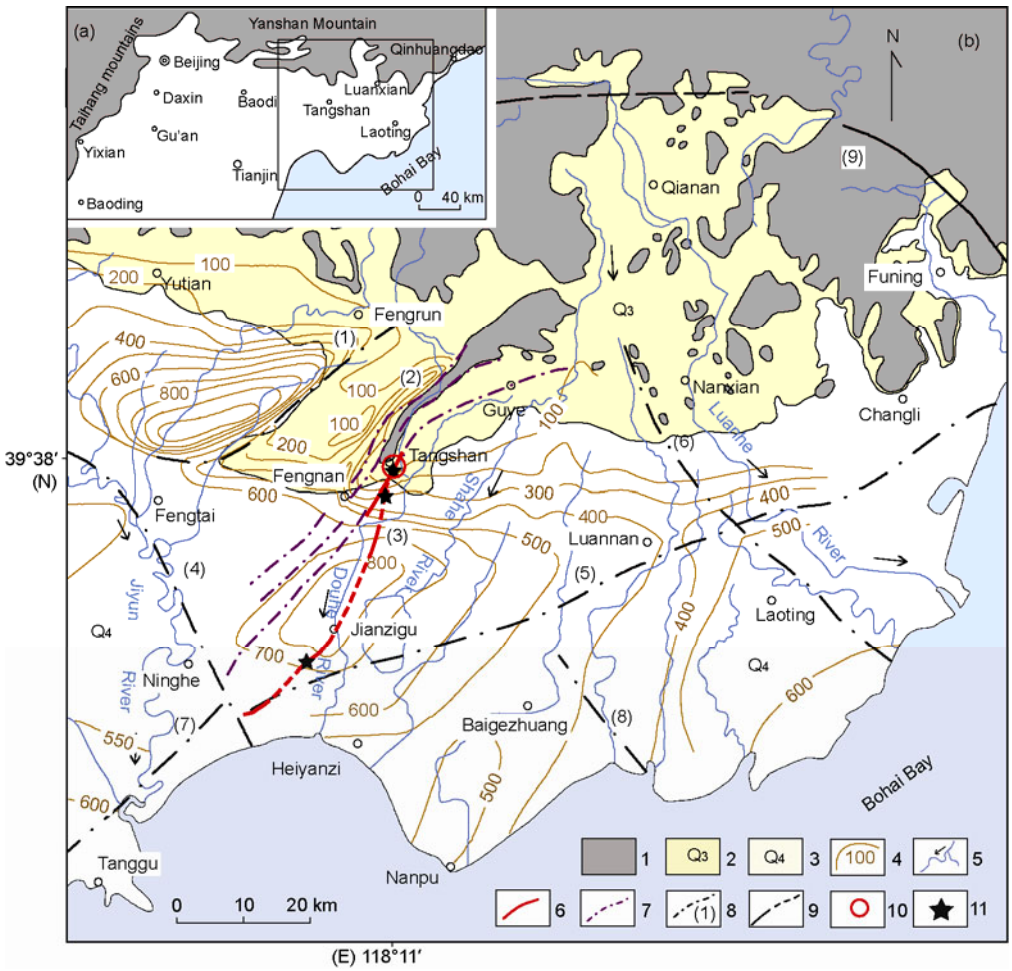

Figure 1 Distribution of the Quaternary system and faults in the Tangshan area (adapted from Liu et al. [28], the distribution of faults was modified slightly). (a) Position of the research place in region; (b) distribution of the Quaternary system and faults in the Tangshan area. 1, Bedrock; 2, Upper Pleistocene sediment; 3, Holocene sediment; 4, isopach of Quaternary in m; 5, river and flow direction; 6, surface rupture zone of the Tangshan 1976 M_s7.8 earthquake; 7, Tangshan fault; 8, buried fault and code: (1) Yejituo Fault, (2) Tangshan Fault, (3) surface rupture zone of the 1976 earthquake, (4) Ji-canal Fault, (5) Ninghe-Changli Fault, (6) Luanxian-Leting Fault, (7) Tanggu Fault, (8) Bogezhuang Fault, (9) Qian'an North Fault; 9, fault and presumption fault; 10, epicenter of the 1976 M_s7.8 earthquake; 11, composite borehole profile of this study.

zone started in the north from Shengli Rd. in Tangshan city, and extended southward in a multiple left-stepping *en echelon* style to the vicinity of Anjizhai. The rupture was about 8 to 11 km long and was dominated by right-lateral strike slip with a maximum displacement of 1.5–2.3 m. The vertical displacements in most sections were 0.2-0.7 m. Wang et al. [3] agreed that the major surface rupture zone was as described above; however, they also considered that the rupture zone might extend discontinuously for 90 km, and on the east and west side of this zone they proposed secondary rupture zones with vertical displacements of several centimeters.

In the present study, we have re-investigated the surface ruptures of the 1976 Tangshan earthquake. At two locations, Tangshan Tenth High School and Niumaku on Kangbai Road, the ruptures have been actively preserved as seismic ruins (Figure 2(a), (b)). Additionally, surface rupture relics can still be seen at Jixiang Road in Tangshan city, in Lishang village, Nuzhizhai town, northwest of Sunjialou of Daodi town, and in Xihe village, Fengnan County (Figure 2(c)).

The following two issues are particularly important to consider. First, previous work [3, 5] and the present study all indicate that the rupture zone from Shengli Road to Anjizhai splits into eastern and western branches south of Lishang village. The eastern branch extends from Lishang village southward, crosses national road No. 205, then passes through the northwest of Sunjialou; the vertical displacement is up on the east and down on the west. The western branch extends from north of Anjizhai southward, and in this case the vertical displacement is up on the west and down on the east. We consider the eastern branch to be the main rupture zone, because the downward throw of the NW side of the east branch is 0.7–0.8 m, accompanied by a right-lateral displacement of 0.9 m [3], whereas although the right-lateral displacement of the west branch is 0.7 m [3],

Figure 2 Earthquake relics and cores recovered from boreholes photos at Niumaku. (a) Earthquake relic at former Tangshan Tenth High School. The surface rupture offset a trail right-laterally, west side up, camera to east. (b) Earthquake relic at Niumaku on Kangbai Road in Tangshan. The tree line is twisted by the rupture zone, west side up, camera to north. (c) Earthquake scarp south of Lishang village in Tangshan, camera to NE. (d) Core array from borehole DZK1-7 at Niumaku. The strata are mainly yellow and yellowish gray in color; the ratio of loam and sandy loam to silty sand is 1∶1. (e) Core samples from depths of 17–19.2 m in borehole DZK1-10 at Niumaku. The loam contains carbon specks. On the right is silty sand. (f) A straight fault plane dipping 75° appears in the brown clay at depths of 33.4–3.9 m in borehole DZK1-8 at Niumaku; there is a thin layer of sand on the fault plane.

its SE side subsided by only about 0.15 m. Second, in this study we connect the previously mentioned [3, 5, 28] Xihe and Fuzhuang ruptures with the Sunjialou and west Lishang ruptures to define a unified zone that has the common displacement feature of up on west and down on east, and possibly an *en echelon* distribution style, such as the left-stepping configuration along Lishang village to Sunjialou. Therefore, the length of the surface rupture zone of the 1976 Tangshan earthquake reaches more than 47 km long. This rupture zone consists mainly of north and south branches.

The north branch starts on the west side of Fuxing Road in Tangshan city, crosses the Tenth High School and Niumaku, and extends discontinuously to the north of Anjizhai; it is about 11 km long and dominated by right-lateral strike-slip accompanied by some vertical displacement up on west and down on east. The south branch extends along West Lishang village, Sunjialou, Xihe, and Fuzhuang with a total length of about 41 km. The displacement is mainly up on east and down on west, accompanied by right-lateral strike-slip. These two ruptures are parallel and have left steps about 1 km apart in the area around Sunjialou-Lishang village; the overlapping length is about 5 km. This overlapping area is also the pivot point of vertical displacement in the surface rupture zone of the 1976 Tangshan earthquake. The instrument-determined epicenter of that earthquake is near this site. Table 1 lists the locations of partial investigation sites of the rupture zone.

The three composite borehole profiles undertaken in this study are located at Niumaku on Kangbai Road on the north branch of the rupture zone, and at Sunjialou in Daodi town and Xihe village in Fengnan County on the south branch. The trench is located at Sunjialou (Figure 3).

2 Investigation of composite borehole profiles

2.1 Brief introduction to the method

In recent years, the composite borehole profiling technique has been increasingly used to detect buried faults in plain areas [29–34]. Borehole investigations are common in geological surveys. Because the objective of an active fault investigation is usually loose sediment, the distance between boreholes in a composite borehole profile must be small and the core taken ratio needs to be high. In the following, we briefly introduce some important ideas for such studies.

The basic principle behind the restoration of fault activities from stratification is the theory of accumulation and superposition, which deals with the configuration and sequence of strata [35]. When describing the active features of a normal fault in a basin, a fault that ruptures and receives sediments simultaneously in a sedimentary environment is called a synsedimentary fault [36]. In the present study, the observed phenomena of thickened strata on downcast walls and an increase of throw with depth are consistent with the expected characteristics of synsedimentary faults. In the

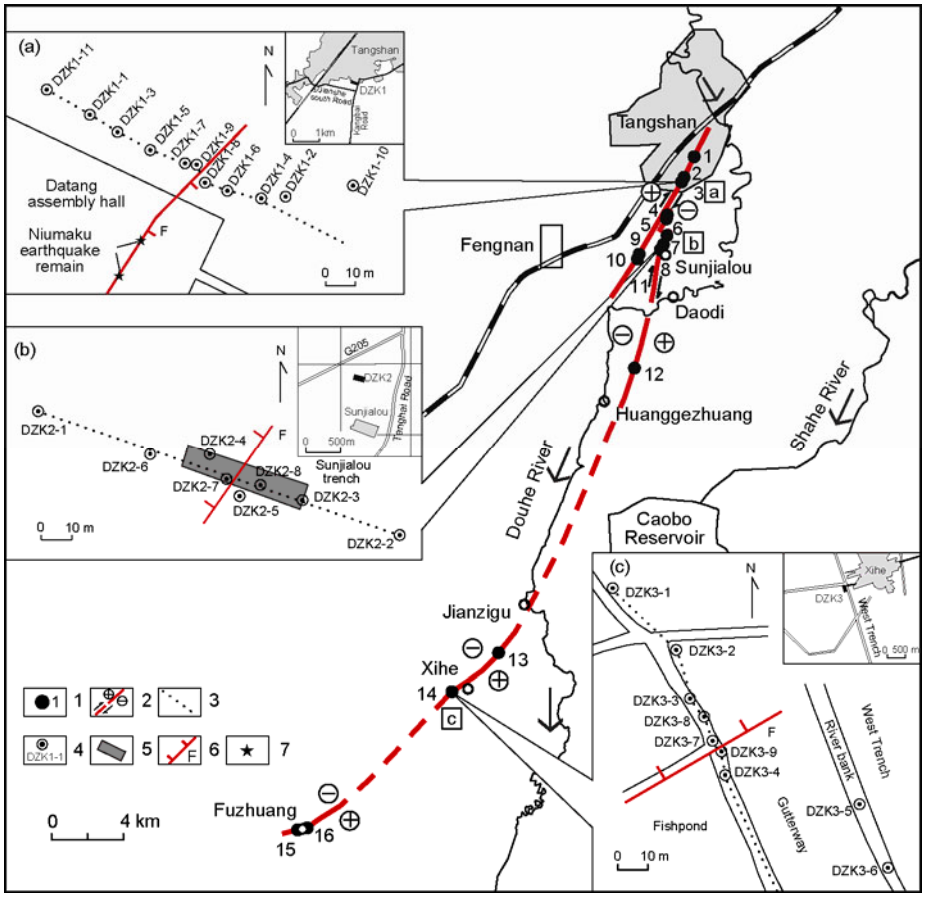

Figure 3 Map of the surface rupture zone of the 1976 Tangshan earthquake indicating the borehole profiles and trench. (a) Borehole layout of Niumaku profile; (b) borehole and trench layout of Sunjialou profile; (c) borehole layout of Xihe profile. 1. Surface rupture site of the 1976 Tangshan earthquake, site number is the same as in Table 1; 2, fault movement, plus sign stands for rising wall, minus sign for sinking wall; 3, borehole profile; 4, borehole number; 5, Sunjialou trench; 6, fault confirmed by borehole or trench; 7, earthquake remains of the 1976 Tangshan earthquake.

Table 1 Field investigation sites along the surface rupture zone of 1976 Tangshan earthquake[a)]

No.	Site	Location	Ground deformation	Notes
1	Remains of Tenth High School	39°36.418′N, 118°11.846′E	Trail right lateral offset 1.2 m, SE side down 0.5 m	Earthquake relic site of Tangshan
2	Jixiang Rd	39°35.791′N, 118°11.453′E	Tree line right lateral offset 1.25 m	Still seen today
a	North of Niumaku	39°35.664′N, 118°11.364′E	Cavity in borehole, stratum offset	Fault passes through the borehole profile here
3	Niumaku	39°35.653′N, 118°11.360′E	Tree line right lateral offset 1.2 m, Vertical displacement 0.3 m	Earthquake relic site of Tangshan
4	West Lishang village	39°34.649′N, 118°10.801′E	Scarp trending NE40°, NW side down 1 m	The up on east and down on west were mentioned at the sites in Guo et al. [2] Still seen today
5	South of west Lishang	39°34.532′N, 118°10.776′E	Surface rupture in NE40°, NW side down 2.0 m	The surface rupture was mentioned in Wang et al. [3]. Still seen today
6	National highway205	39°34.034′N, 118°10.777′E	Scarp trending NE20°, NW side down 0.5 m then	Identified by local people, no longer exist
7	Sunjialou	39°33.736′N, 118°10.638′E	Ground deformation NE40°–50°, NW side down 0.8 m	Gentle slope is seen at present.
b	Sunjialou trench	39°33.758′N, 118°10.657′E	Fault attitude NE40°/NW∠69°	Passing through Sunjialou trench and borehole profile in this study
8	West of Sunjialou	39°33.594′N, 118°10.533′E	NE-trending scarp and gentle slope in corn field appeared during the earthquake	Identified by Yang Hecheng, the village head of Sunjialou
9	Yufeng Steel Plant	39°33.460′N, 118°09.722′E	Pigsty right lateral offset 15 cm, SE side down 15 cm	Disappeared now
10	North of Anjizhai	39°33.322′N, 118°09.638′E	SE side of crack down 20 cm, disappeared	Mentioned in Guo et al. [2], Yang [4], Du et al. [5] and Wang et al. [3], identified by local people
11	North St. of Anjizhai	39°33.315′N, 118°09.649′E	Dirt road NE30° right lateral offset 70 cm	Still discernable now
12	Haozhuangzi of Huanggezhuang town	39°30.010′N, 118°09.540′E	Sand gushing, cracking, bulging during earthquake	Confirmed by local people
13	Xihe No.1 village, Fengnan County	39°21.355′N, 118°04.288′E	Ground scarp, SE side up 1.7 m	Mentioned in Wang et al. [3], Qiu et al. [25], and Wu [27]. Relics are still seen now. Fault cuts the borehole profile of this study.
14	Xihe No.3 village, Fengnan County	39°20.187′N, 118°02.487′E	NE65° trending, SE side up more than 1 m	
c	Xihe No.3 village, Fengnan County	39°20.187′N, 118°02.487′E	Fault plane confirmed by borehole	
15	Village Council of Fuzhuang	39°16.063′N, 117°56.901′E	Boundary between ground uplift and subsidence	Mentioned in Du et al. [5], Wang et al. [3], and Qiu et al. [25], identified by local people
16	East of Fuzhuang	39°15.999′N, 117°56.534′E	North side down 2.5 m	

a) a, b and c are the three sites of the composite borehole porfiles undertaken in this study; b is also the site of the trench in this study.

study of active faults, besides the ruptures of strata, the difference of displacement at different depths should also be watched, so as to help judge the occurrence of multi-stage activities and to infer the time of activity from the age of the strata.

In active fault studies, the frequently mentioned term "event" refers to a fault activity discernable in time based on broken strata and relief. In a stratigraphic section, the resolving power for events is restricted by the number of discernable displacement data. The displacement datum of a single event can be called the "event marker stratum", which is the newest stratum broken by a single event and is distinguishable from the effect of later events. In a stratigraphic section containing multiple stages of fault activity, the vertical displacements of strata increase stepwise from top downward and from young to old. That is, the displacement of strata deposited during the quiet stage of fault activity is the same as that of the newest stratum broken by later fault activity, but different from the displacement of the strata broken by earlier activity [35]. By stripping the vertical displacements from young to old strata and using the ages of the newest stratum among the strata with the same displacement and the age of cover stratum, we can count fault events and infer the time of activity. In brief, the number of dip-slip events on a stratigraphic section is roughly equal to the ratio of the cumulative displacement of the strata to the average displacement of individual events.

2.2 Outline of profiles

Three borehole profiles, 4 and 27.5 km apart from each other, were established at Niumaku, Sunjialou, and Xihe (Figure 3). The total number of boreholes in the three profiles is 28, and the total drilling footage is 1217 m. Core diameter is 97–110 mm, taken every 2.0 m. The ratio of coring of silk, sandy clay and clay reaches to more than 90%. The ratio of coring of fine and middle sand reaches to 60%–80%. The ratio of coring of coarse and gravel reaches to less than 40%.

The Niumaku profile is located on the north side of the earthquake remains site at Niumaku (Figure 3(a)). It trends NW65°, with 11 boreholes within 101 m distance. The borehole depth is 25.4–35.4 m, maximum borehole spacing 17 m, minimum spacing 4.0 m, total footage 333 m. The

Sunjialou profile was accomplished before the excavation of Sunjialou trench. The profile trends NW55°, with 8 boreholes over a 124 m distance, the borehole depths are 30.0–61.5 m, maximum spacing 39 m, minimum spacing 6.0 m, and total footage 436 m. Boreholes DZK2-4, 7, 5, and 8 are located at the site of the trench (Figure 3(b)). The Xihe profile is situated on the west of Xihe village (Figure 3(c)), trending NW15°, with 9 boreholes over a distance of 128 m; the borehole depth 31.0–61.4 m, maximum spacing 32 m, minimum spacing 5.0 m, and total footage 448 m. The above three profiles all cross the surface rupture zone of the 1976 Tangshan earthquake.

2.3 Stratification and dating

(1) Niumaku profile. The strata revealed by this profile can be divided into 13 layers in five sets of varying thicknesses, which can be compared between boreholes (Figure 4). The upper 0.9–1.4 m is cultivated soil and backfill. Below that, Set I of the strata is dominated by sandy loam with loam appearing at the bottom. It includes Layers 2 and 3 and is 4–8 m thick. Set II contains silty sand or medium-to-fine-grained sand and is 5–6 m thick. It consists of Layer 4. Set III is loam and clay with silt, about 5–7 m thick, consisting of Layers 5, 6, and 7. Set IV contains mainly silty sand. The NW section of the profile has a certain amount of sandy loam, which increases in the SE section. This set of strata is about –7.9 m thick and includes Layers 8 and 9. Set V is composed of loam, clay, sandy loam and silt strata, and appears only in the NW section of the profile. Its thickness is about 5–9 m and it includes Layers 10 to 13. In this profile, the thickness ratio of loam-sandy loam to silty sand-medium coarse sand is about 1∶1 (Figure 2(d)). The ages of 15 samples from this profile have been measured.

The stratigraphic sequence at Niumaku borehole profile is described as follows:

Layer 1. Cultivated soil at the ground surface.

Layer 2. Sandy loam, with loam locally; the thermoluminescence (TL) dating results of two samples from this layer are 46.76±3.97 and 49.79±4.23 ka B.P.

Layer 3. Loam and clay, mixed with grayish brown clay lumps in some boreholes. TL dating of two samples from this layer gives ages of 41.43±3.53 and 54.49±4.63 ka B.P.

Layer 4. Medium-fine sand, or silty sand and medium-to-coarse-grained sand and sandy loam, loam in a few boreholes. One TL dating sample has an age of 52.40±4.15 ka.

Layer 5. Sandy loam, or loam and silty sand in a few boreholes. Two TL dating samples have ages of 49.50±4.21 and 57.60±4.89 ka.

Layer 6. Medium-fine sand, silty sand.

Layer 7. Clay and loam (Figure 2(e)).

Layer 8. Silty sand and medium-fine sand. Two TL dating samples have ages of 59.64±5.07 and 67.90±5.77 ka.

Layer 9. Sandy loam in upper part, silty sand in lower part. Two TL dating samples have ages of 75.18±6.30 and 74.75±6.35 ka.

Layer 10. Clay and loam. The age of one TL sample is 75.95±6.46 ka.

Layer 11. Silty sand, or sandy loam with clay in a few boreholes. The age of one TL sample is 103.60±8.81 ka.

Layer 12. Clay, loam and sandy loam, silt. The age of one TL sample is 114.99±9.77 ka.

Layer 13. Sandy loam, or loam in some boreholes. The age of one TL sample is 110.17±9.36 ka.

Stratum dating from this profile is listed in Table 2.

(2) Sunjialou profile. The strata in this profile can be divided into 20 layers in four sets, which can generally be compared between boreholes (Figure 5). Set I lies from the surface to a depth of 4–5 m. It consists mainly of loam and sandy loam and includes Layers 1 and 2. Set II is silty sand with some medium-to-coarse-grained sand. It is about 14 m thick and includes Layers 3 to 7, among which Layer 6 is sandy loam. Set III consists of interbedded loam, sandy loam, and silty sand, but loam dominates. The set is about 20 m thick and includes Layers 8 to 12. Set IV has the coarsest grains in this profile, consisting mainly of medium-to-fine-grained sand and coarse-grained sand. The set is about 25 m thick and includes Layers 13 to 20, among which Layers 15, 17, and 19 are thin layers of loam and sandy loam. The thickness ratio of loam and sandy loam to silty sand and medium-to-coarse-grained sand in the profile is about 1∶2 (Figure 6(a)). 13 TL dating samples from this profile have been measured.

The strata sequence in Sunjialou profile is as follows:

Layer 1. Surface cultivated soil.

Layer 2. Sandy loam and loam with lime nodules.

Layer 3. Fine sand and silt. The age of two TL samples is 41.62±3.54 and 55.59±4.72 ka.

Layer 4. Loam and sandy loam, most boreholes can be seen.

Layer 5. Medium-to-coarse- and fine-grained sand.

Layer 6. Sandy loam. The age of two TL samples is 59.05±5.02 and 63.25±5.38 ka.

Layer 7. Silty sand with medium-grained sand locally.

Layer 8. Loam with clay and sandy loam locally.

Layer 9. Silty sand with medium-grained sand locally.

Layer 10. Clay and loam.

Layer 11. Silty sand with sandy loam locally. Two TL samples show ages of 79.96±6.79 and 92.22±7.84 ka; the latter seems too old as compared with the upper and lower layers.

Layer 12. Clay with sandy loam locally.

Layer 13. Silty sand with medium-to-coarse-grained sand locally. Two TL samples result in ages of 109.47±9.30 and 79.58±6.67 ka; the former seems too old as compared with the upper and lower layers.

Layer 14. Pebbles and sandy loam. The diameter of larger pebbles reaches 5 cm. Well rounded (Figure 6(b)). One TL sample gives an age of 103.97±8.84 ka.

Layer 15. Clay with loam and sandy loam locally. One TL sample gives an age of 132.94±11.30 ka, which is too old as compared with the age of the lower layer.

Layer 16. Silty sand with medium-to-fine-grained sand locally.

Layer 17. Sandy loam with clay locally.

Layer 18. Silty sand. One TL sample gives an age of 114.92±9.77 ka.

Table 2 Dating results of samples from the boreholes and trench at three sites in Tangshan[a)]

No.	No. of borehole or trench	Sample No.	Depth (m)	Layer	Lithology	Age (ka BP)
Niumaku Profile						
1	Dzk1-4	TL-1	6.8	Layer 2	Yellow sandy loam	49.79±4.23
2	Dzk1-9	TL-1	4.4	Layer 2	Brownish red sandy loam	46.76±3.97
3	Dzk1-8	TL-1	6.9	Layer 3	Yellowish brown loam	41.43±3.53
4	Dzk1-6	TL-1	6.8	Layer 3	Grayish brown mixed clay	54.49±4.63
5	Dzk1-9	TL-2	6.3	Layer 4	Yellow sandy loam	52.40±4.15
6	Dzk1-9	TL-3	10.5	Layer 5	Yellow sandy loam	49.50±4.21
7	Dzk1-8	TL-2	14.2	Layer 5	Yellow loam	57.60±4.89
8	Dzk1-7	TL-2	15.6	Layer 8	Yellowish gray mottled sandy loam	59.64±5.07
9	Dzk1-8	TL-3	23.0	Layer 8	Yellow fine sand	67.90±5.77
10	Dzk1-8	TL-4	27.0	Layer 9	Yellow silt	74.75±6.35
11	Dzk1-3	TL-2	21.5	Layer 9	Yellowish gray sandy loam	75.18±6.30
12	Dzk1-2	TL-4	28.2	Layer 10	Yellowish brown clay	75.95±6.46
13	Dzk1-7	TL-3	26.8	Layer 11	Grayish yellow silty sand	103.60±8.81
14	Dzk1-9	TL-5	32.6	Layer 12	Grayish yellow sandy loam	114.99±9.77
15	Dzk1-3	TL-3	29.1	Layer 13	Brownish gray silty sand	110.17±9.36
Sunjialou Profile						
16	Dzk2-1	TL-3	11.3	Layer 3	Yellowish gray silty sand	55.59±4.72
17	Dzk2-4	TL-2	10.5	Layer 3	Gray silt	41.62±3.54
18	Dzk2-7	TL-1	13.8	Layer 6	Yellow sandy loam	63.25±5.38
19	Dzk2-6	TL-2	15.1	Layer 6	Grayish yellow sandy loam	59.05±5.02
20	Dzk2-7	TL-3	29.0	Layer 11	Yellowish brown silt	92.22±7.84
21	Dzk2-4	TL-4	31.3	Layer 11	Yellowish gray silty sand	79.96±6.79
22	Dzk2-6	TL-5	41.2	Layer 13	Yellowish gray silty sand	79.58±6.67
23	Dzk2-4	TL-5	38.8	Layer 13.	Yellowish gray silty sand	109.47±9.30
24	Dzk2-7	TL-4	40.9	Layer 14	Yellow sandy loam	103.97±8.84
25	Dzk2-5	TL-5	44.2	Layer 15	Silt with sandy loam	132.94±11.30
26	Dzk2-4	TL-6	50.8	Layer 18	Gray silty sand	114.92±9.77
27	Dzk2-4	TL-7	57.9	Layer 20	Yellowish gray medium fine sand	126.64±10.76
28	Dzk2-7	TL-5	56.5	Layer 20	Yellow medium fine sand	117.22±9.96
Xihe Profile						
29	Dzk3-6	TL-1	5.1	Layer 3	Grayish black sandy loam	6.12±0.52
30	Dzk3-8	TL-1	5.2	Layer 3	Grayish black sandy loam	8.13±0.69
31	Dzk3-1	^{14}C-1	5.25	Layer 3	Grayish black sandy loam	11.625±0.13
32	Dzk3-2	B^{14}C-1-O	7.0	Layer 3	Grayish black silk	8.07±0.04
33	Dzk3-2	B^{14}C-1-P	7.0	Layer 3	Grayish black silk	6.54±0.04
34	Dzk3-4	^{14}C-1	12.5	Layer 4	Grayish black clay	11.92±0.12
35	Dzk3-8	TL-2	17.0	Layer 5	Gray sandy loam	13.51±1.15
36	Dzk3-4	TL-2	18.7	Layer 5	Gray loam	14.57±1.24
37	Dzk3-6	TL-3	22.9	Layer 6	Yellow sandy loam	23.88±2.03
38	Dzk3-8	TL-3	27.2	Layer 6	Yellow sandy loam	24.21±2.06
39	Dzk3-3	TL-1	33.0	Layer 7	Brownish yellow clay	26.57±2.26
40	Dzk3-2	^{14}C-3	33.0	Layer 7	Grayish black clay	28.11±0.535
41	Dzk3-4	TL-4	35.8	Layer 8	Yellowish gray silty sand	47.58±4.04
42	Dzk3-5	TL-2	37.0	Layer 8	Yellow fine sand	48.83±4.15
43	Sunjialou trench	TL-6	0.65	Layer 2	Yellow loam with tiny lime nodule	7.61±0.65
44	Sunjialou trench	^{14}C-2	2.15	Layer 3	Grayish brown clay	5.734-6.215
45	Sunjialou trench	TL-8	2.4	Layer 3	Grayish yellow loam	17.62±1.50
46	Sunjialou trench	ESR	2.1	Layer 4	Pale lime nodule	25±2
47	Sunjialou trench	TL-9	3.1	Layer 8	Yellow loam	27.57±2.34
48	Sunjialou trench	TL-3	3.0	Layer 4	Yellow loam with abundant lime nodule	31.45±2.67
49	Sunjialou trench	B^{14}C-1-O	3.2	Layer 5	Gray and orange sandy loam	12.56±0.05
50	Sunjialou trench	TL-2	3.5	Layer 6	Yellowish brown sandy loam	33.53±2.85
51	Sunjialou trench	TL-1	4.5	Layer 7	Light-yellow fine sand	34.91±2.97

a) ^{14}C and ESR dating was done by the Key Laboratory of Earthquake Dynamics of the Institute of Geology, CEA; TL dating by the Geologic Chronology Laboratory of the Institute of Crustal Dynamics, CEA; B^{14}C dating was done by the Beta Analytic Radiocarbon Dating Laboratory, USA, In them, B^{14}C-O dating was done by organic sediment in sample and B^{14}C-P dating was done by plant material in sample.

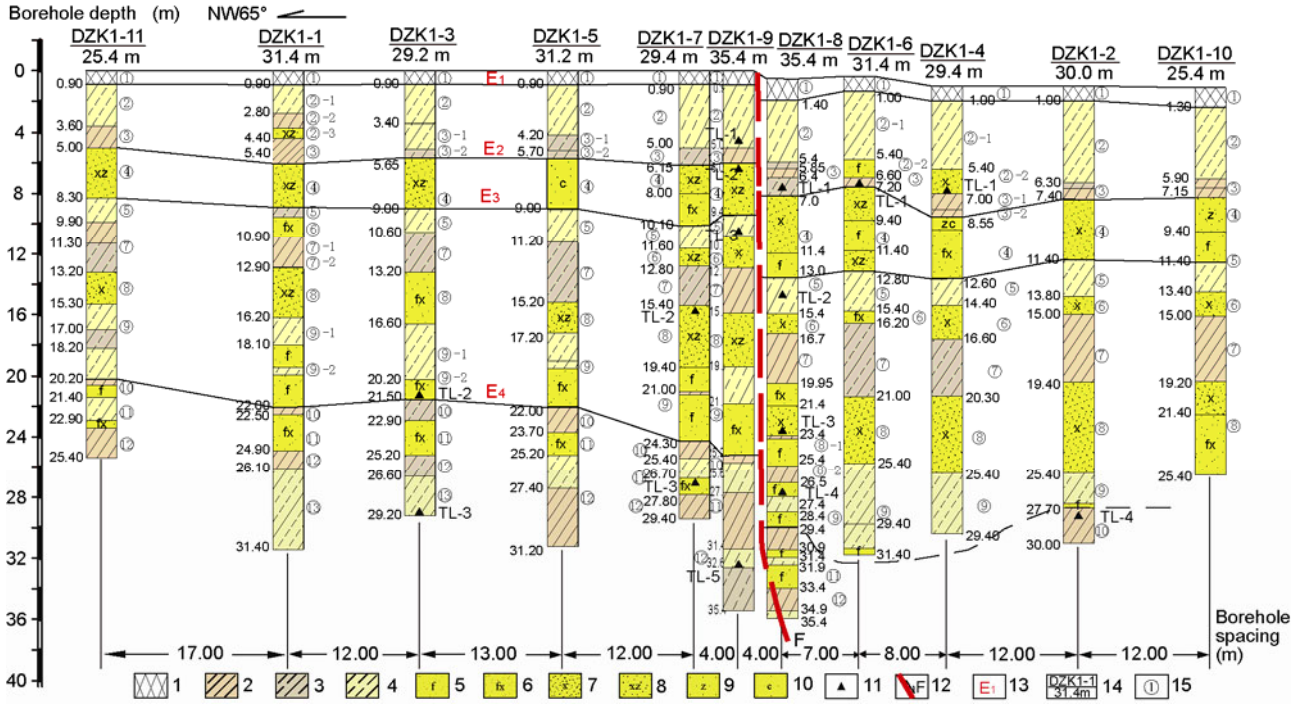

Figure 4 Niumaku composite borehole profile. 1, Surface disturbed soil; 2, clay; 3, loam; 4, sandy loam; 5, silt; 6, silty sand; 7, fine sand; 8, medium fine sand; 9, medium sand; 10, coarse sand; 11, TL sampling site; 12, fault; 13, dividing of earthquake events; 14. serial number of borehole and largest depth of borehole; 15, stratum number.

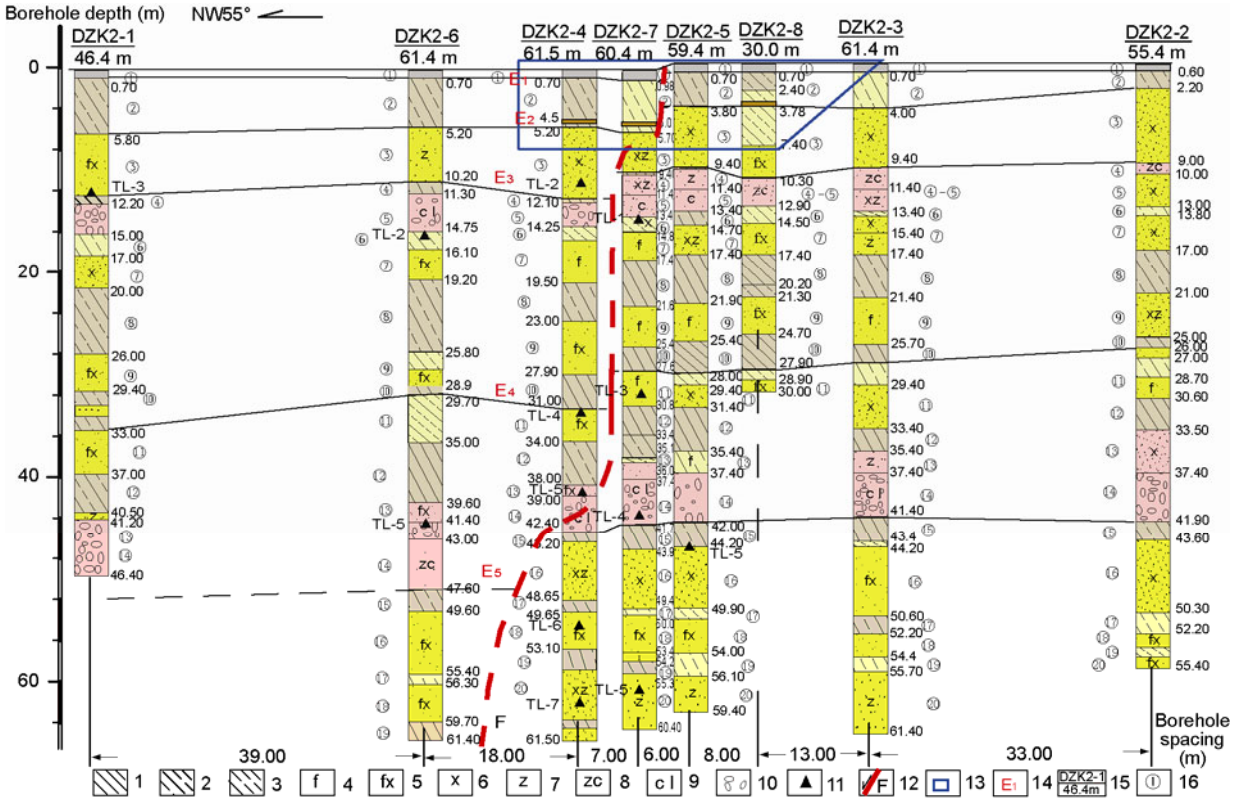

Figure 5 Sunjialou composite borehole profile. 1. Clay; 2, loam; 3, sandy loam; 4, silt; 5, silty sand; 6, fine sand; 7, medium sand; 8, medium fine sand; 9, coarse sand-gravel; 10, gravel; 11, TL sampling site; 12. fault, 13. trench location; 14. dividing of earthquake events; 15. serial number of borehole and largest depth of borehole; 16, stratum number.

Figure 6 The Sunjialou and Xihe cores recovered from the boreholes photos and the Xihe Tangshan earthquake aerophoto. (a) Core array from borehole DZK2-7 at Sunjialou. The color of strata is mainly yellow and yellowish gray. The ratio of loam and sandy loam to silty sand is 1∶2. (b) Cores from 35.4–39.0 m in borehole DZK2-7 at Sunjialou. The arrow in middle indicates the boundary between sandy loam and fine-grained sand strata. The upper arrow points to gravels contained in fine-grained sand, which are well rounded and of variable composition. (c) Cores from 53.4–59.4 m in borehole DZK2-5 at Sunjialou. (d) 1∶10000 aerial photo of Xihe village, Fengnan County, taken after the 1976 Tangshan earthquake. Arrow indicates the scarp to the west of Xihe, plus side up, minus side down. (e) Core array from borehole DZK3-5 at Xihe. The color of strata is alternatively grayish black and yellow, the ratio of loam and sandy loam to silty sand is 1∶1. (f) Abundant biologic fragments in brownish yellow sandy loam at 27.4–29.4 m in borehole DZK3-5 at Xihe.

Layer 19. Sandy loam with mud layers.

Layer 20. Silty sand and medium-to-fine-grained sand (Figure 6(c)). Two TL samples result in ages of 126.64±10.76 and 117.22±9.96 ka.

(3) Xihe profile. Xihe profile is located at Tangshan earthquake scarp trending. The strata in this profile can be divided into 11 layers in four sets, which can be generally compared between boreholes (Figure 7). Unlike the previous two profiles, this profile contains a number of gray mud layers, which indicate a carbon-rich still-water sedimentary

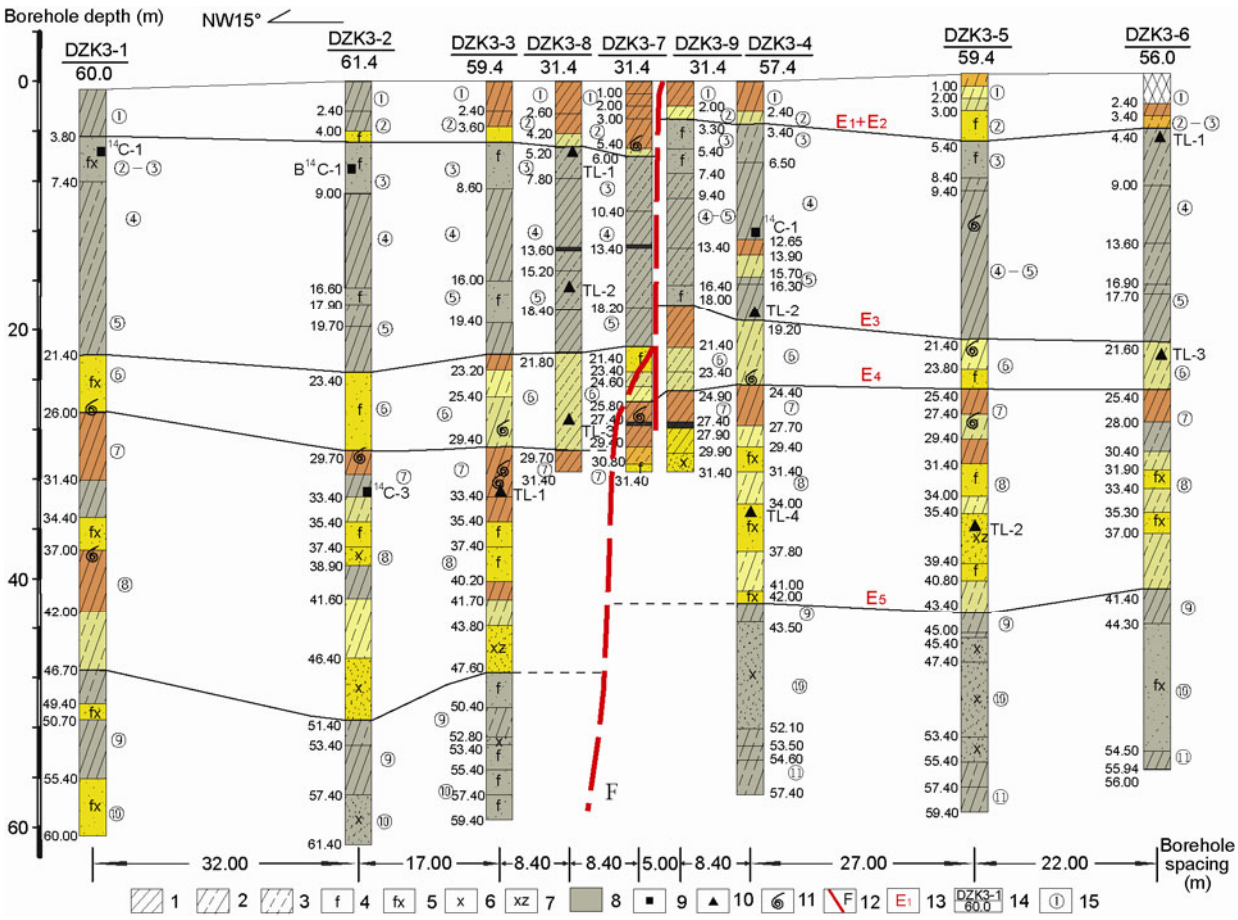

Figure 7 Xihe composite borehole profile.1, Clay; 2, loam; 3, sandy loam; 4, silt; 5, silty sand; 6, fine sand; 7, medium fine sand; 8, black peat, blackish gray or geayish green clay; 9, ^{14}C sampling site; 10, TL sampling site; 11, biologic calcareous fragments; 12, fault; 13, dividing of earthquake events; 14, serial number of borehole and largest depth of borehole; 15, stratum number.

environment. For stratigraphic comparison in this profile we took into account the color of each stratum. The color in these four stratum sets is alternatively grayish yellow and gray. The 5–6 m below the surface are Set I. This set generally consists of brown clay, but it is grayish brown in a few boreholes, and includes Layers 1 and 2. Set II is composed of grayish black clay and loam with some grayish black silty sand and sandy loam. It includes Layers 3 to 5 and is 14–18 m thick. Set III consists of yellow silt, yellowish gray clay and sandy loam. It includes Layers 6 to 8 and is about 20–28 m thick. Set IV is dominated by gray silty sand with some sandy loam, loam, and clay. It consists of Layers 9 to 11, and is about 10–16 m thick. In this profile the thickness ratio of gray strata to yellow strata and that of fine-grained strata, such as sandy loam and loam to silty sand, are all about 1∶1 (Figure 6(e)). 14 dating samples from this profile were measured.

The stratigraphic sequence of the Xihe profile is as follows:

Layer 1. Grayish brown and brown clay. In some boreholes the top 0.5 m is backfill.

Layer 2. Grayish yellow-yellowish gray sandy loam and silty sand locally.

Layer 3. Grayish black silt and sandy loam. Two TL dating samples result in ages of 6.12±0.52 and 8.13±0.69 ka. One ^{14}C sample gives an age of 11.625±0.13 ka. The other ^{14}C sample is done by AMS method. Tow results are obtained. One gives an age of 8.07±0.04 ka from dating of organic sediment of sample. The other gives an age of 6.54±0.04 ka from dating of plant material of sample.

Layer 4. Grayish black muddy loam and clay. ^{14}C dating of one sample gives an age of 11.92±0.12 ka.

Layer 5. Grayish black muddy loam and clay, with silt and sandy loam in some boreholes. A very few boreholes contain biologic fragments. Two TL samples show ages of 14.57±1.24 and 13.51±1.15 ka.

Layer 6. Yellow silt and sandy loam. Biologic fragments are seen in a number of boreholes (Figure 6(f)). Two TL dating samples result in ages of 23.88±2.03 and 24.21±2.06 ka.

Layer 7. Brown clay and loam, gray locally, biologic fragments seen in a number of boreholes. The results of one TL dating and one ^{14}C dating give 26.57±2.26 and 28.11±0.535 ka, respectively.

Layer 8. Grayish yellow silty sand, with clay in boreholes DZK3-1, 2, and 3. Two TL dating samples give ages of 47.58± 4.04 and 48.83±4.15 ka.

Layer 9. Gray silty sand and sandy loam in some boreholes; loam and clay in other boreholes.

Layer 10. Gray silty sand and medium-to-fine-grained sand,

with sandy loam locally.

Layer 11. Seen in the SE part of the profile only, consisting of sandy loam, loam, and clay.

(4) Sedimentary environment and age of strata. From the lithology of the above three boreholes, it is known that the strata in the Niumaku (DZK1) and Sunjialou (DZK2) profiles south of Tangshan city consist of sediments of an alluvial-proluvial plain, dominated by silty sand, sandy loam, and loam, whereas the strata of the Xihe profile (DZK3) in southernmost Fengnan County consist of sediments from a littoral plain.The Niumaku and Sunjialou profiles are 4 km apart. Although the thickness of the second set of strata (II) at Sunjialou is three times that at Niumaku, the first set of sandy loam strata and the second set of silty sand strata of these two profiles are comparable. Further down, the strata of Sets III, IV, and V in the Niumaku profile can be compared with those of Set III in the Sunjialou profile. Both are composed of interbedded silty sand, sandy loam, and clay, except that a set of gravel-bearing coarse sand at the top of Set III in the Sunjialou profile is not found in the Niumaku profile. The third set of strata in the Xihe profile consists of interbedded silty sand, sandy loam, and loam, This set contains abundant biologic fragments, probably indicating a relatively large-scale transgression of the Bohai Sea in the late stages of the Late Pleistocene.

The isopach contours of the Quaternary system in the Tangshan area trend generally in a near-EW direction. The thickness of the Quaternary system increases from 100 m in the north to 600 m in the south [27]. Controversy exists as to the age of the Late Quaternary strata in the Tangshan area. Chen and Ni [37] considered that the thickness of Holocene series is greater than 20 m to the south of Tangshan city but less than 20 m to the north, and suggest that the thickness of the upper Pleistocene series to the south of Tangshan is 75–150 m. On the other hand, on the geologic map of the Tangshan area[1)], the strata to the south and north of Tangshan city are respectively marked as Holocene and Upper Pleistocene. The dating results of this study are close to the regional geologic map. That is, to the south of Tangshan city, the strata 4–6 m below the surface are from the middle stage of the Late Pleistocene, whereas around Xihe in Fengnan County, the thickness of the Holocene series reaches 10–13 m.

2.4 Faulting events

(1) Niumaku profile. In the Niumaku composite borehole profile, the 13 strata consisting of sandy loam, loam, and silty sand are sediments of an alluvial-proluvial plain. The distribution of strata in this profile indicates that their original orientation was near-horizontal within a distance of several to tens of meters. As seen in Figure 4, the east side of all strata dropped between boreholes DZK1-9 and DZK1-8 with throws varying from 0.5–6.2 m (Table 3). By considering the throw of the same strata between boreholes DZK1-5 and DZK1-8, then the maximum throw of this profile is 8.7 m.

In the reference frame of stratum dislocation, the identification of marker layers directly affects the determination of occurrence times for related event. Theoretically, the dislocation character of a synsedimentary fault is that the throw of an upper layer of a dip-slipping fault is less than that of a lower layer. However, considering the errors in borehole depths recorded during the process of drilling and core recovery, as well as the complexity resulting from strike-slip motions, it is possible for individual layers that the throw of an upper layer could be greater than that of a lower layer. However, this phenomenon should occur for only a very few layers and does not affect the overall analysis of the events. Based on the criterion that a marker layer is the youngest layer broken by a single event that is distinguishable from a later event, the top of layer 1 (the ground surface) and the bottoms of layers 3, 4, and 9 were selected as the marker layers for four faulting events in the Niumaku profile. These events are analyzed as follows in order of increasing age.

Between boreholes DZK1-9 and DZK1-8 on this profile, the ground surface has a vertical throw of 0.5 m, which resulted from the surface displacement caused by the 1976 Tangshan earthquake (event E_1). Table 1 shows that the vertical displacement at the Niumaku earthquake remains, 30 m south of this profile, is 0.3 m. The vertical displacements caused by the Tangshan earthquake at these two sites are similar. Putting boreholes DZK1-9 and DZK1-8 at the same elevation coordinate scale, the vertical throw of the marker layers for three other events is as follows. The throw of the bottom of Layer 3 at a depth of 6–7.5 m is 1.5 m. That of the bottom of Layer 4 at 9.4–13.5 m is 4.1 m, and that of the bottom of Layer 9 at 25.2–29.9 m is 4.7 m. These values all include the throw caused by the 1976 Tangshan earthquake (event E_1). They exist not only between these two boreholes, but also extend to both sides through the entire profile. Layer 3 is the marker for event E_2, which occurred after the sedimentation of the bottom of Layer 3 and caused a vertical displacement of 1.0 m. After that, loam accumulated in borehole DZK1-8 on the descending wall and silty sand accumulated in boreholes DZK1-6 and 4, which were not found in the nearby boreholes. The 4.1 m throw of the bottom of marker Layer 4 for event E_3 includes the vertical displacement of events E_3, E_2, and E_1. After deducting the displacement of the previous two events, the vertical displacement of event E_3 is determined to be 2.6 m. The 4.7 m throw of the top of the event E_4 marker layer 10 includes the displacement of four events E_1–E_4. After deducting the displacements of the previous three events, the vertical displacement of event E_4 is found to be 0.6 m. On

1) Geological Bureau of Hebei Province. 1∶200000 Regional Geologic Map of Tangshan. 1977

Table 3 Depth and displacement of faulted strata in Tangshan three sites profiles[a)]

Niumaku profile DZK1		Sunjialou profile DZK2		Xihe profile DZK3	
Depth of faulted layer[**]	Throw and event	Depth of faulted layer	Throw and event	Depth of faulted layer	Throw and event
DZK1-9–DZK1-8 Bottom of Layer 1 0.9–1.9 m Bottom of Layer 2 5.0–5.9 m	1976 M_s7.8 E_1, D_1=0.5 m	DZK2-5–DZK2-7 Bottom of Layer 1 0.7–1.0 m	1976 M_s7.8 E_1, D_1=0.8 m	Bottom of Layer 1 DZK3-9–DZK3-7 * Bottom of Layer 2 3.3–6.0 m	1976 M_s7.8 E_1+E_2, D_{1+2}=2.7 m E_1, D_1=1.3 m E_2, D_2=1.4 m
DZK1-9–DZK1-8 * Bottom of Layer 3 6.0–7.5 m	E_2, D_{2+1}=1.5 m D_2=1.0 m	DZK2-5–DZK2-7 * Bottom of Layer 2 3.8–5.7 m	E_2, D_{1+2}=1.9 m D_2=1.1 m		
DZK1-9–DZK1-8 * Bottom of Layer 4 9.4–13.5 m	E_3, D_{1+2+3}=4.1 m D_3=2.6 m	DZK2-7–DZK2-4 * Bottom of Layer 3 9.4–12.1 m	E_3, D_{1+2+3}=2.7 m D_3=0.8 m	DZK3-9–DZK3-7 * Bottom of Layers 4–5 18.0–21.4 m	E_3, D_{1+2+3}=3.4 m D_3=0.7 m
DZK1-9 – DZK1-8 * Bottom of Layer 9 25.2–29.9 m	E_4, $D_{1+2+3+4}$=4.7 m D_4=0.6 m	DZK2-7–DZK2-4 * Bottom of Layer10 27.6–31.0 m	E_4, $D_{1+2+3+4}$=3.4 m D_4=0.7 m	DZK3-9–DZK3-8 * Bottom of Layer 6 24.9–29.7 m	E_4, $D_{1+2+3+4}$=4.8 m D_4=1.4 m
DZK1-5–DZK1-8 Bottom of Layer 9 22.0–29.9 m	$D_{1+2+3+4}$=7.9 m D_4=3.8 m				
DZK1-9–DZK1-8 Bottom of Layer 10 25.6–31.4 m	D=5.3 m	DZK2-4–DZK2-6 * Bottom of Layer 14 42.4–47.6 m	E_5, $D_{1+2+3+4+5}$=5.2 m D_5=1.8 m	DZK3-4–DZK3-3 * Bottom of Layer 8 42.0–47.6 m	E_5, $D_{1+2+3+4+5}$=5.6 m D_5=0.8 m
DZK1-5–DZK1-8 Bottom of Layer 10 23.7–31.4 m	D=7.7 m			DZK3-4–DZK3-2 Bottom of Layer 8 42.0–51.4 m	D_5=4.6 m
DZK1-9–DZK1-8 Bottom of Layer 11 27.7–33.9 m	D=6.2 m	DZK2-4–DZK2-6 Bottom of Layer 15 43.2–49.6 m	D=6.4 m	DZK3-4–DZK3-3 Bottom of Layer 9 43.5–52.8 m	D=9.3 m
DZK1-5–DZK1-8 Bottom of Layer 11 25.2–33.9 m	D=8.7 m	DZK2-4–DZK2-6 Bottom of Layer 16 48.1–55.4 m	D=6.7 m	DZK3-4–DZK3-2 Bottom of Layer 9 43.5–57.4 m	D=13.9 m

a) * means marker layer of an event. ** means that 0.5 m is added to the depth of each layer in the boreholes on the lowered wall (east of DZK1-8), so as to adjust the elevation of borehole mouth to the same level.

the NW side of borehole DZK1-9, Layer 10 is raised by 3.2 m in borehole DZK1-5, then the layer is generally horizontal. However, on the SE side of DZK1-8, clay Layer 10 is not seen, indicating that it is buried at a deeper depth on the SE side of borehole DZK1-8. Comparing the throw of Layer 10 between boreholes DZK1-5 and DZK1-8, the vertical displacement of this event was found to reach 3.8 m. Further down, the throws on Layers 10 and 11 are 5.8 and 6.2 m, respectively, between boreholes DZK1-9 and DZK1-8, and 7.7 and 8.7 m between boreholes DZK1-5 and DZK1-8. However, because layers 9 and below are not shown in boreholes DZK1-6 and DZK1-4 to the east of borehole DZK1-8, we do not discuss these further here.

In addition to the stratal dislocations described above, a flat fault plane dipping 70° appeared in the clay core at a depth of 33.6 m in borehole DZK1-8. A thin layer of fine sand exists on the fault plane (Figure 2(f)). The occurrence of the fault plane agrees with the stratal discontinuity observed between the two boreholes above, indicating that the fault passes through borehole DZK1-8 and extends between boreholes DZK1-9 and DZK1-8. Because the distance between DZK1-9 and DZK1-8 is only 4 m, the dip angle of the fault above a depth of 33 m should be greater than 80°, i.e. nearly upright.

During the fieldwork undertaken to construct this profile, two more boreholes were tried between DZK1-8 and DZK1-9 in an attempt to encounter the fault plane. However, when the two holes were drilled to 7.4 m below the surface, severe mud leakage in the borehole walls forced drilling to stop. This is related to the fact that the fault passes through this point.

(2) Sunjialou profile. The 20 layers in this profile are dominated by silty sand, with some medium-to-coarse-grained sand intercalated with sandy loam and clay, indicating the nature of the alluvial plain sedimentation. The lithology is generally comparable among the boreholes, and the strata are nearly horizontal in the profile. However, between DZK2-6 and DZK2-4, DZK2-4 and DZK2-7, and DZK2-7 and DZK2-5, westward throw exists in deep to shallow strata, indicating the existence of a steep, west-dipping fault. In this profile, the top of Layer 1, the bottoms of Layers 2, 3, 10, and 14 are the markers for five faulting events, and Layer 1 drops were caused by the 1976 Tangshan earthquake (Figure 5).

Between boreholes DZK2-5 and DZK2-7, the west side of the bottom of Layer 2 drops by 1.9 m. Such a throw continues to both the east and west. At depths of 3.65–3.78 m in borehole DZK2-8, a thin layer of mixed orange and grayish black sandy loam is observed. In borehole DZK2-7 and DZK2-4 this layer is seen at depths of 5 m and 4.3–4.38 m, respectively. Considering that there is an elevation difference of 0.5 m between the borehole openings of DZK2-8

and DZK2-7, then the 1.85 m throw of the thin orange and grayish black sandy loam is basically consistent with the 1.9 m throw of the bottom of Layer 2. Layer 2 was faulted by event E_2. After deducting the 0.8 m vertical displacement caused by the 1976 Tangshan earthquake at this site, the displacement of event E_2 is found to be 1.1 m. The vertical displacements of Layers 3 and 10 between DZK2-7 and DZK2-4 and that of Layer 14 between DZK2-4 and DZK2-6 are respectively 2.7 m, 3.4 m, and 5.2 m. After deducting the throws caused by later events, the vertical displacements of events E_3, E_4, and E_5 are 0.8, 0.7, and 1.8 m, respectively. The throws of Layers 15 and 16 between DZK2-4 and DZK2-6 are 6.4 m and 6.7 m, respectively. Because of severe mud leakage of the coarse sand-gravel layer in borehole DZK2-1 to the west of DZK2-6, the strata below Layer 14 were not extracted, and are not discussed further.

Figure 5 and the above descriptions show that the fault passes from bottom upward between boreholes DZK2-6 and DZK2-4, DZK2-4 and DZK2-7, then between DZK2-7 and DZK2-5, dipping NW at an angle of about 60°.

(3) Xihe profile. The Xihe profile is divided into 11 layers and is characterized by the occurrence of grayish black muddy strata that occupy nearly half of the total thickness. Lithologies consists of sandy loam, loam, silt, and medium-to-fine-grained sand. The grayish yellow sandy loam and clay between the grayish black muddy strata contain abundant biologic fragments. For stratal comparisons, the dark muddy strata serve as the marker layers. Figure 7 shows that the lithologies of strata correlated between the boreholes are generally comparable. The fault passes from the bottom upward between boreholes DZK3-3 and DZK3-4, DZK3-8 and DZK3-7, then between DZK3-7 and DZK3-9, dipping to the west at 70°–80°. In this profile, the markers for five faulting events are the top of layer 1 (the ground surface), and the bottoms of Layers 1, 5, 6, and 8.

At the location of this profile, the land has been recultivated several times since the 1976 Tangshan earthquake, and ground deformation caused by the earthquake is no longer obvious. However, several hundred meters to the west of this profile, a residual 1.1-m-high scarp can still be seen. According to the statements of villagers, at the site of this profile, the 1976 earthquake induced a vertical throw of about 1.3 m on the ground surface. Figure 7 shows that the west side of the bottoms of Layers 2 and 5 between boreholes DZK3-7 and DZK3-9, the bottom of Layer 6 between DZK3-8 and DZK3-9, and the bottom of Layer 8 between DZK3-3 and DZK3-4 dropped by 2.7, 3.4, 4.8, and 5.6 m, respectively. After deducting the previous throws, the vertical displacements of event E_2 to E_5 were respectively 1.4, 0.7, 1.4, and 0.8 m. In addition, the bottom of layer 9 has a throw of 9.3 m between DZK3-4 and DZK3-3 and a throw of 13.9 m between DZK3-4 and DZK3-2, which will not be discussed here.

In addition to the above phenomena, the strata of this profile have two other significant features. First, Layers 6 and 7, consisting of yellow sandy loam and clay with abundant biologic fragments, are marker layers in this profile, which have been offset together with other layers. Second, at the bottom of Layer 6, at depths of 24.6–25.8 m in borehole DZK3-7, there are mixed yellowish gray silt and loam, with the latter containing silt lumps. This is related to event E_4 of the fault on the SE side of the borehole, and maybe is the accumulation mixture on the descending wall.

2.5 A comparison of faulting events on the three profiles

(1) Depth of marker layers and division of events. Using only the depths of marker layers to compare faulting events in the three profiles, the four faulting events identified in the 30 m deep boreholes of the Niumaku profile can be compared with the youngest four of the five events identified in the 60 m deep boreholes of the Sunjialou and Xihe profiles. The 1976 Tangshan earthquake is manifested in the top layer of both the Niumaku and Sunjialou profiles, whereas its impact is not seen in the Xihe profile due to artificial disturbances. Event E_2, which preceded the 1976 earthquake, is seen at the depths of 5–7 m below the surface in all three profiles; earlier event E_3 is seen at 9–13 m in the Niumaku and Sunjialou profiles and at 18–21 m in the Xihe profile. Event E_4 is seen at depths of 25–29 m in the Niumaku profile, consistent with observational depths of 27–31 and 25–30 m in the Sunjialou and Xihe profiles, respectively. Event E_5 is seen at 42–47 m in both the Sunjialou and Xihe profiles (Figure 8(a)). These data show that there is a relationship between the depth of a marker layer and the fault activities along the three profiles.

(2) Stratum dating and timing of faulting events. In the Xihe profile, prior to the Tangshan earthquake, event E_2 broke the top of Layer 3. Three dating samples of the layer were taken from the ends and middle of the profile. Ages determined by ^{14}C and TL dating are 11.6 and 8.13 ka, respectively, so the earthquake therefore occurred after 8.13–11.6 ka B.P. Event E_3 took place after Layer 6 and before Layer 5, i.e. before 14.57 ka and after 23.88 ka B.P., denoted as 14.57–23.88 ka and should be rather close to 14.57 ka. Event E_4 occurred before Layer 6 and after Layer 7; ages determined by one ^{14}C and three TL samples are respectively after 28.11 ka, 26.57 ka, before 24.21 ka and 23.88 ka B.P., denoted as 24.21–26.57 ka BP. These dating results show that, when counting with the minimum age of each event or with the median value of the time span of each event, the recurrence intervals of the four events including the 1976 Tangshan earthquake are as follows. The interval between E_1 and E_2 is 8.13 or 9.86 ka; the interval between E_2 and E_3 is 6.44 or 9.365 ka; the interval between E_3 and E_4 is 9.64 or 6.165 ka. On average, the recurrence interval of the latest activities of Tangshan Fault in Late Quaternary is about 6.165–9.86 ka.

In the Niumaku and Sunjialou profiles, event E_1 is the ground deformation caused by the 1976 Tangshan earthquake. E_2 is an event prior to the 1976 Tangshan earthquake. Because the trench in the Sunjialou profile afforded more dating results, we shall discuss the timing of event E_2 at this location later. In the Niumaku profile, if only considering the age of stratum broken by each event, the age of strata broken by E_2 is 41.43–52.40 ka, that of E_3 is 52.40–57.60 ka, and that of E_4 is 75.18–103.60 ka. The interval between E_2 and E_3 is 8.07 ka, and the interval between E_3 and E_4 is 34.39 ka with the median value of the time span. In the Sunjialou profile, the age of the strata broken by events E_3 to E_5 is, respectively, 55.59–59.05, >79.96, and 103.97–114.92 ka. The minimum age of recurrence interral between E_3 and E_4, E_4 and E_5 is 24 ka or 20–30 respectively. We have calculated the average time interval of fault activities from the ratio of cumulative vertical seismic displacement to the displacement of a single event. In the Niumaku profile, Layer 9 with an age of 75.18 ka has been offset by 4.7 m (E_4), indicating that there have been nine events with a vertical displacement of 0.5 m; hence the average interval of fault activities is 8.4 ka. In the Sunjialou profile, Layer 14 with an age of 103.97 ka has a throw of 5.2 m (E_5), so the average interval of events with an average displacement of 0.7–0.8 m is 14.9 ka. The Xihe profile shows that the recurrence interval of the four faulting events since the late stage of Late Pleistocene is 6.165–9.86 ka. The minimum time and vertical displacement of each event in the above three profiles are shown in Figure 8(b).

The above data indicate that in the last stage of Late Pleistocene, the region around Tangshan was being eroded. If only the division of earthquake events in age of strata, the events E_2 to E_4 of Niumaku and Sunjialou profiles happened 4 million years ago, like Figure 8(b) shows. But from the co-seismic displacement analysis, the author thinks earthquake events that Figure 8(a) shows belong closer to the truth. Namely, the three profiles reveals that the latest 4 paleoseismic events are synchronize activities. Niumaku and Sunjialou profiles did not have the sedimentary after the late stage of Late Pleistocene, activities of these two profiles

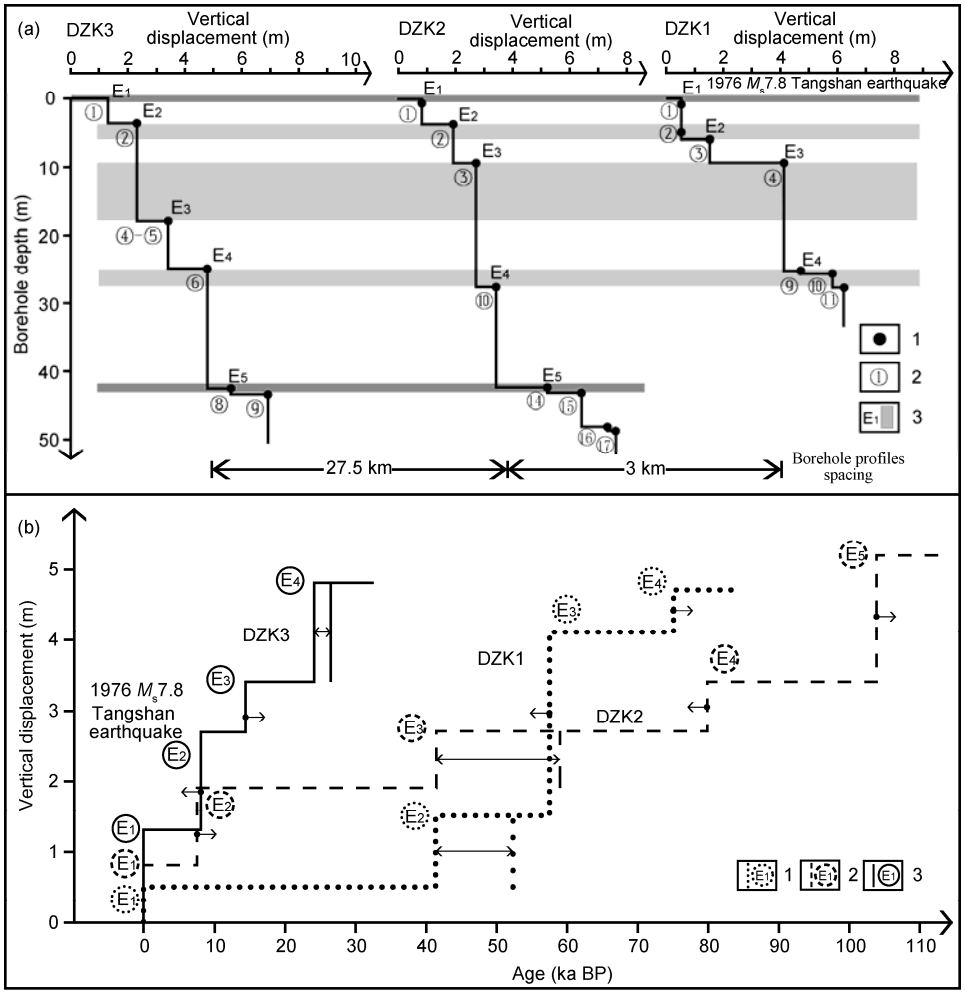

Figure 8 Depths of marker layer, occurrence times of events, and vertical displacements in the Tangshan composite borehole profiles. (a) Relationship of marker layer depths and vertical displacements: 1. Depth and displacement of each event; 2, marker layer of an event; 3, division of events. (b) Relationship of event time and vertical displacement: 1, Division of events in profile DZK1; 2, division of events in profile DZK2; 3, division of events in profile DZK3.

during this period hidden in the displacement of early strata. Namely, when the surface was being eroded in the last stage of Late Pleistocene, faulting activities broke the latest morphologic unit, but the stratigraphic age was older than the age of morphologic unit obviously. From the above data can be seen that the comparison of faulting events between the depth of the strata and the co-seismic displacement is more reasonable.

(3) Intensity of activity. The above data indicate that the vertical ground displacement caused by the 1976 M_s7.8 Tangshan earthquake was, respectively, 0.5, 0.8 m, and 1.3 m at the Niumaku, Sunjialou, and Xihe profiles. Before the 1976 Tangshan earthquake, the vertical displacement was 0.6–2.6 m for each of the three events in the Niumaku profile, 0.7–1.8 m for each of the four events in the Sunjialou profile, and 0.7–1.4 m for each of the four events in the Xihe profile. They are all similar to or greater than the vertical ground displacement caused by the 1976 Tangshan M_s7.8 earthquake at each site. We infer that the earthquake magnitudes corresponding to these events were therefore equivalent to that of the 1976 earthquake.

3 Sunjialou trench

The Sunjialou trench is located about 500 m northwest of Sunjialou village, Daodi town, on the alluvial-proluvial plain to the south of Tangshan city. At this location there is an ~70-cm-high, NE45°-trending gentle slope, that is high in the SE and low in the NW, which corresponds to the surface scarp of the 1976 Tangshan earthquake (Figure 9(a)), subsequently smoothed by farming. The layout of Sunjialou trench considered the geometry of the surface rupture zone of 1976 earthquake, as well as the result of the borehole investigations presented in this study. The trench spans boreholes DZK2-4, 7, 5, and 8 of the Sunjialou profile, and borehole DZK2-3 is at the east end of the trench (Figure 5). The trench trends in a NW65° direction, is 35 m long, 7 m wide at the top, 1.5 m wide at the bottom, and 6.2 m deep (Figure 9(b)). As mentioned above, among the four boreholes, three of them contain the orange stratum defined as layer 5 in the trench section. The throw of layer 2 in the borehole profile agrees with the measured throw in the lower part of the trench.

3.1 Strata and dating

This trench revealed seven strata (Figure 10), which are all fine-grained sediments. There is fine-grained sand and sandy loam in the bottom part of the trench, and loam with calcareous nodules in the middle and upper part. For correspondence with the strata in the boreholes, the strata in the trench were numbered from top downward. One ^{14}C, six TL, and one electron spin resonance (ESR) samples from the trench were measured.

The strata in the trench are described as follows.

Layer 1. Grayish black loam and cultivated soil, with mixed local accumulations of yellow sand and clay lumps.

Layer 2. Yellow loam containing calcareous nodules with diameters ⩽0.5 cm. The age determined from sample TL-6 from the top of this layer in the SE section of the trench is 7.61±0.65 ka BP.

Layer 3. Grayish yellow loam without calcareous nodules but with grayish brown clay lumps. The ^{14}C dating result of this layer is 5.21±0.24 ka BP.; its corrected value is 5.734–6.215 ka BP.; the age determined from sample TL-8 from the bottom of this layer is 17.62±1.50 ka BP. This layer appears in the NW section of the trench and on the descending wall only. Near to the fault, the bottom of this layer slopes.

Layer 4. Grayish yellow loam with abundant calcareous nodules generally with diameters 1–3 cm, but occasionally as high as 10–15 cm. The bottom part contains a large quantity of tiny carbon particles. The age determined from the base of sample TL-3 is 31.45±2.67 ka BP. The layer is 1.8 m thick on the rising wall and 2.2 m thick on the descending wall. Scattered clay lumps occur near the fault plane. The ESR dating result for a calcareous nodule from this layer is 25±2 ka BP.

Layer 5. Thin layer of gray and orange sandy loam, generally 5–7 cm, occasionally 10 cm thick. The dating of the B^{14}C-1-O sample is 12.56±0.05 ka BP. by AMS.

Layer 6. Yellowish brown sandy loam with a discontinuous, thin layer of gray sandy loam about 5 cm thick. The layer contains no calcareous nodules but a large quantity of carbon or manganese particles. The dating result of sample TL-2 from the top of the layer is 33.53±2.85 ka BP.

Layer 7. Pure light-yellow fine-grained sand with clear horizontal bedding. The dating result of sample TL-1 from the top of the layer is 34.91±2.97 kaBP.

Layer 8. Gray loam distributed near the fault plane. The shape of the layer resembles the fill in a tensile crack. The dating result of sample TL-9 from this layer is 27.57±2.34 ka BP.

3.2 Faulting phenomena

The faulting phenomena revealed by the Sunjialou trench are as follows.

(1) In the middle section of the lower part on the north wall of the trench there are four parallel faults seen in a 4-m-wide section. Among them, the attitude of the fault on the east (F_1) is trending NE46°, dipping NW at an angle of about 69°. This fault extends from the lower part upwards to the top of the trench, and has broken all strata except for the present cultivated soil on the surface (Figure 9(c), (d)). On the NW side of the fault the bottom of Layer 1 drops 0.7–0.8 m, and Layer 5 drops 0.8 m. The attitude of the three faults on the west (F_2–F_4) is trending NE15°, dipping NW at an angle of about 73°. They broke Layers 5 to 7 only in the lower part of the trench, making layer 5 stagger from east to west with a throw of 0.7 m (Figure 9(e)). The fault configuration on the south wall of the trench is similar, also with four faults within 3 m. However, the three parallel faults (F_2–F_4) in the lower part of the section are on the east side of the major fault, rather on its west side (Figure 10).

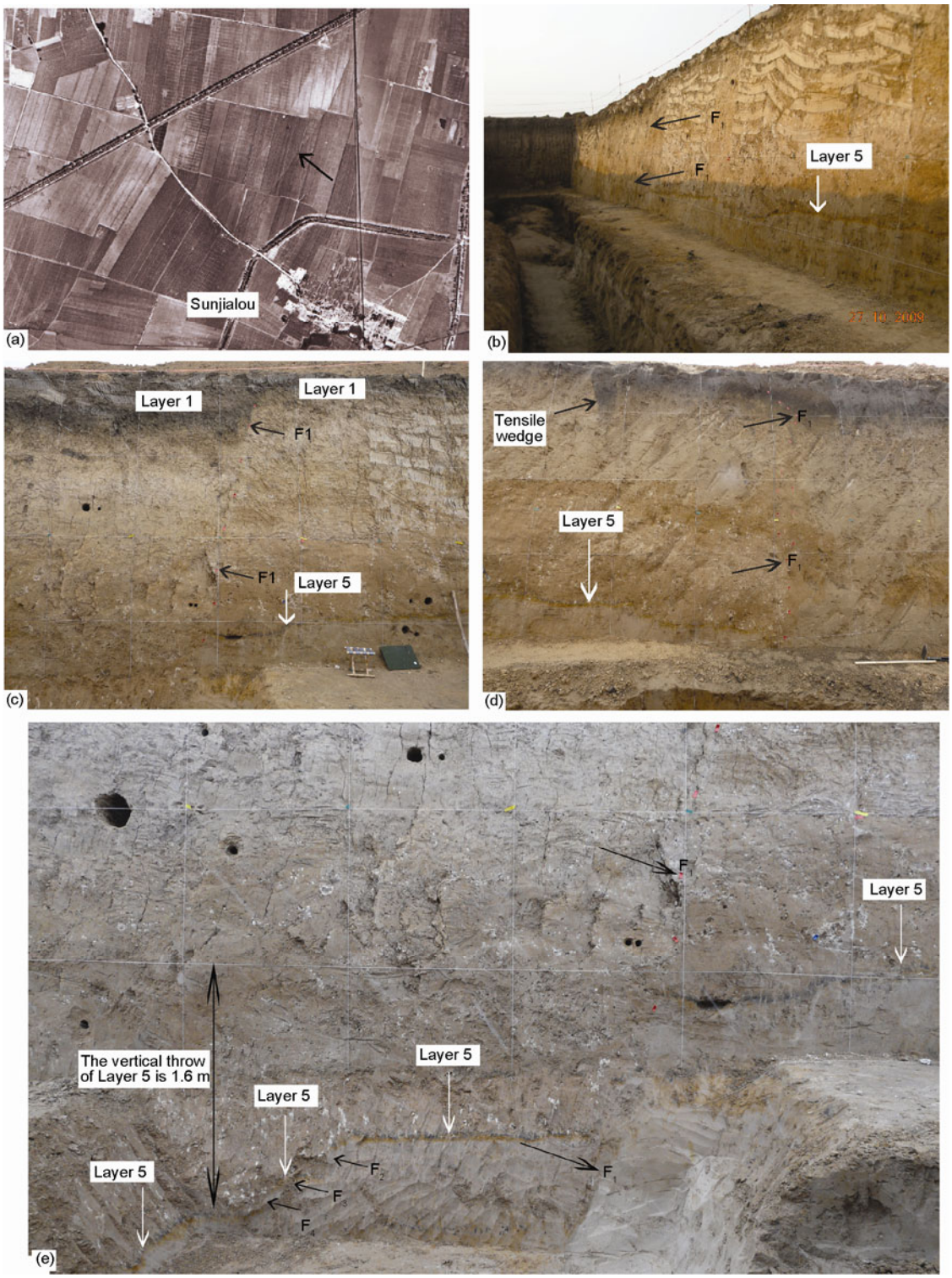

Figure 9 The Sunjialou Tangshan earthquake aerophoto and the Sunjialou trench photos. (a) The surface rupture zone at Sunjialou in a 1∶10000 aerial photo taken after the 1976 Tangshan earthquake. (b) A view of the Sunjialou trench, camera to NE. (c) A section of offset soil and lower strata on the northern wall of Soujialou trench. The layer marked as 5 is the thin black and orange sandy loam distributed on the rising wall, camera to NE. (d) A section of tensile wedge and offset strata in the upper part of the southern wall of Sunjialou trench. Layer 5 is a thin black and orange sandy loam layer distributed on the rising wall, camera to SW. (e) The lower section of the north wall of Sunjialou trench and the throw of strata. The vertical throw of Layer 5 is 1.6 m as marked in the lower part of the photo. Grid spacing in the photo is 1 m, camera to NE.

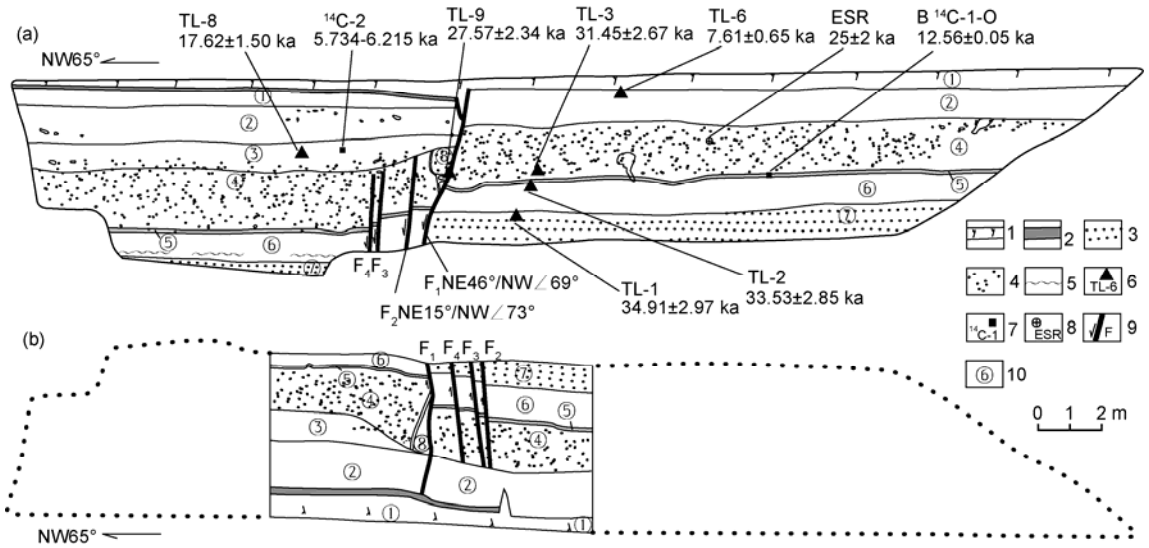

Figure 10 Section of Sunjialou trench. (a) North wall of the trench; (b) south wall of the trench. 1, Present ground surface; 2, ancient ground; 3, fine sand; 4, loam with calcareous nodules; 5, ground water layer; 6,TL dating; 7, ^{14}C dating; 8, ESR dating; 9, fault and number;10, stratum number.

(2) Tensile black-loam-filled cracks appear near the ground surface in both the north and south wall of the trench. The tensile cracks in the north wall are located on the major fault plane (F_1), whereas those in the south wall are on the rising wall of the fault, about 2 m away from the major fault. Furthermore, on the descending walls of the major fault, on both walls in the middle part of the trench, there are near-vertical clay stripes about 5 cm wide. These stripes are probably early-stage tensile-torsional cracks (Figure 10(a), (b)), where the loam was turned into clay due to friction [38, 39], or they also could be stripes of different hue caused by micro-cracks in the vicinity of the major fault plane [40].

(3) The thickness of Layer 4 is about 1.8 m on the east side of the fault belt, and about 2.2 m on the west; the difference is 0.4 m. Layer 3 only occurs on the west side of the fault and is about 0.4 m thick. This increased thickness of Layer 4 on the west side of the fault plus the thickness of Layer 3 equals the vertical dislocation of Layer 5 caused by faults F_2 and F_3 on the west side of the major fault.

Therefore, from the faulting phenomena in the Sunjialou trench described above, we know that the fault had at least two rupture events. The most recent one was the 1976 Tangshan earthquake (E_1). It is seen from the trench section that the bottom of Layer 1 on the west of the fault is thicker than that on the east by 0.7–0.8 m. Over the years since the 1976 Tangshan earthquake, the surface scarp of the fault has been smoothed, covering the black loam originally on the surface of the west side of the fault by a mixed layer. In the trench section, the tensile wedge below the surface and the throw of the major fault plane were both caused by the 1976 Tangshan earthquake.

The earlier activity of this fault is manifested by the following phenomena. First, the vertical displacement of layer 5 in the lower part of the trench is twice that of layers 1 and 2 in the upper part. Stripping the throw of the upper stratum from the greater throw of lower stratum, there should be a faulting event that occurred between the two sets of strata. Furthermore, the thickening of Layer 4 and the occurrence of Layer 3 on the west side of the fault, the mixed accumulation on top of Layer 5, as well as the fact that faults F_2–F_4 did not extend into Layer 3 and upper layers, are all consistent with a fault rupture resulting from fault throw stripping. That is, faulting occurred after the sedimentation of layer 4, resulting in F_2–F_4, the vertical clay stripes on the west side of F_1, as well as the vertical dislocation in Layer 4 and lower layers. Later, Layer 3 and the mixed accumulation on top of Layer 4 were formed from erosional processes in that location.

Note also that, based on the distribution and occurrence of fault F_1 and F_2–F_4 on the two sides of the trench, the fault belt F_2–F_4 of earlier event E_2 trends NE15°, whereas F_1 of the later event E_1 trends NE46° and cuts F_2–F_4.

3.3 Time of faulting

In addition to constraining the 1976 Tangshan earthquake, this trench also revealed an earlier faulting event. In the section, the throws of Layer 5 and the top of layer 4 are basically the same, indicating that the earlier event occurred after the deposition of layer 4. The TL and ESR dating results of layer 4 are respectively 31.45±2.67 and 25±2 ka BP. The B^{14}C-1-O dating result of Layer 5 by AMS is 12.56±0.05 ka BP. The accumulation layer on Layer 4 on the descending wall of the fault should roughly indicate the cover layer age of the event. The corrected ^{14}C dating result of the grayish brown clay lump in Layer 3 is 5.734–6.215 ka; whereas the result from the TL sample is 17.62±1.50 ka.

The TL sample from the cover Layer 2 gives an age of 7.61±0.65 ka. The discrepancy of these dating results may be related to the rather long period of denudation and erosion after the formation of Layer 4. However, the preserved accumulation shape of Layer 3 means that this event occurred recently. Therefore, we set the time of the earlier faulting event as before 7.61±0.65 ka BP. Recalling that the time of E_2 on Xihe profile is after 8.13 ka BP., so the occurrence time of this event is about 7.61–8.13 ka BP.

4 Discussion and conclusion

(1) The data from three composite borehole profiles and a trench south of Tangshan city indicate that the surface rupture zone of the 1976 M_s7.8 Tangshan earthquake extends southward, passing by the west side of Sunjialou, Daodi town in Fengnan County, to Xihe in Fengnan County, with a length greater than 47 km.

(2) The investigation on the 1976 earthquake showed that the north branch of the surface rupture zone starts from Shengli Road in Tangshan city, passes through the Tenth High School and Niumaku on Kangbai Road on the west side of Fuxing Road in Tangshan city, and extends southward to Wangmatai; the vertical displacement is up on the west and down on the east. The south branch of the surface rupture zone starts from Lishangzhuang and passes southward through Sunjialou and Xihe; the vertical displacement is up on east and down on west. Such a faulting mode cannot be explained by normal faulting or reverse faulting alone, but is consistent with the vertical displacement field caused by right-lateral strike-slip faulting. Fault throw on strata characterized by drilling and trenching have confirmed that such a faulting mode persisted during the Late Quaternary.

(3) The present study indicates that multiple rupture events occurred on the Tangshan fault belt in the Late Quaternary. Prior to the 1976 Tangshan earthquake, the latest three events occurred at 7.61–8.13, >14.57 ka, and 24.21–26.57 ka BP. Together with the 1976 earthquake, the four events have recurrence interval of about 6.7–10.8 ka with the median value. In the Niumaku profile, a 75.18-ka- old stratum indicates that the average interval of nine events is 8.4 ka. These data showed the activity mode of Tangshan fault in the Late Quaternary as a quasi-periodic recurrence of large earthquakes. The recurrence interval of strong earthquakes here is 2.5 times that of the Xiadian fault (3.3 ka), which is also located in the northern part of North China Plain and has produced the 1679 *M*8 Sanhe, Hebei earthquake [41].

(4) The study of three composite borehole profiles showed that the temporal resolution of faulting events on the profile is restricted by the sedimentary environment of the strata. If both sides of the fault were to remain within a depositional sedimentary environment during the period of interests, the event and occurrence time could be determined by making use of event marker strata. If the early loose strata were eroded later, data recovery from the sediments in unlikely. Only average intervals between fault ruptures can be inferred from the ratio of cumulative vertical displacement to single event displacement and the age of strata with cumulative displacement.

(5) This paper has investigated the number and temporal history of activities of Tangshan fault belt in the Late Quaternary based on dividing the accumulated vertical displacement of strata in borehole profiles and a trench section. The Tangshan Fault is only one example of a continental seismogenic strike-slip fault. Further analyses of other strike-slip faults are required to investigate whether their activities can be constrained from differences in vertical displacements.

In the field, Huang Wei participated in core cataloguing and sampling, Huang Wei and Sun Changbin participated in trench excavation, and Sheng Qiang participated in clearing of trench walls. We thank Academician Deng Qidong and Professors Yang Zhuen, Yin Gongming, Qiu Zehua, Lei Jianshe, Yang Shuxin, Li Dewen, Li Dewen, and Ma Baoqi for their guidance and discussions on the Sunjialou trenching site. We are grateful to the valuable comments from Professors Wang Tingmei, Guo Shunmin, and the reviewers of the manuscript. This work wass supported by the Fundamental Research Funds of Institute of Crustal Dynamics, China Earthquake Adminishtration (Grant No. ZDJ2007-1).

1 Li S B. The map of seismicity of China (in Chinese). Acta Geophys Sin, 1957, 6: 127–158
2 Guo S M, Li Z Y, Cheng S P, et al. Discussion on the regional structure background and the seismogenic model of the Tangshan earthquake (in Chinese). Sci Geol Sin, 1977, 12: 3–19
3 Wang J M, Zheng W J, Chen G S, et al. A study on the principal surface fracture belt and the cause of occurrence of the Tangshan earthquake (in Chinese). J Seismol Res, 1981, 4: 437–450
4 Yang L H. Seismic intensity and damage (in Chinese). In: Editorial Group of "the 1976 Tangshan Earthquake", SSB. The 1976 Tangshan Earthquake. Beijing: Seismological Press, 1982. 1–32
5 Du C T, Meng X L, Chen S X. Ground fissures of the Tangshan earthquake (in Chinese). In: Liu H X, ed. Disaster of Great Earthquake (1). Beijing: Seismological Press, 1985. 174–189
6 Chen Y T, Lin B H, Wang X H, et al. A dislocation model of the Tangshan earthquake of 1976 from the inversion of geodetic data (in Chinese). Acta Geophys Sin, 1979, 22: 3–19
7 Butler R, Stewart G S, Kanamori H. The July 27, 1976 Tangshan, China Earthquake—A complex sequence of intraplate events. Bull Seismol Soc Amer, 1979, (69/1): 207–220
8 Li Q Z, Zhang Z L, Jin Y M, et al. Focal mechanisms of Tangshan earthquakes (in Chinese). Seismol Geol, 1980, 2: 61–69
9 Zhang Z L, Li Q Z, Gu J C, et al. The fracture processes of the Tangshan earthquake and its mechanical analysis (in Chinese). Acta Seismol Sin, 1980, 2: 3–21
10 Huang L R. An analysis of the horizontal displacement field of Tangshan earthquake with generalized inverse method and a comparison with the classic method (in Chinese). Crustal Deform Earthquake, 1981, 1: 3–13
11 Zhang Z S, Xie J M, Xu F Z, et al. Vertical deformational associated with the 1976 Tangshan *M*=7.8 earthquake (in Chinese). Acta Geophys Sin, 1981, 24: 58–67
12 Xie J M. Some features of crustal elastic rebound of the Tangshan earthquake (in Chinese). J Seismol Res, 1984, 7: 28–37
13 Shao X Z, Zhang J R, Zhang S Y, et al. Investigation of deep struc-

tures in Tangshan earthquake area (in Chinese). Acta Geophys Sin, 1986, 29: 30–43
14 LI X G. Tectonic features of the plain area of the southern side of Mt. Yanshan and their relations with the Tangshan earthquake (in Chinese). In: Institute of Geology, Chinese Academy of Sciense, Institute of Geology, State Seismological Bureau, eds. Formation and Development of the North China Fault Block Region. Beijing: Science Press, 1980. 261–273
15 Geophysical Exploration Team, State Seismological Bureau. Laoting-Zhangjiakou deep seismic sounding profile (in Chinese). Earthquake, 1977, 2: 13–14
16 Zeng R S, Lu H X, Ding Z F. Seismic refraction and reflection profilings across Tangshan epicentral region and their implication to seismogenic processes (in Chinese). Acta Geophys Sin, 1988, 31: 383–398
17 Liu G D. Research on focus structures and dynamical process of Tangshan earthquake (in Chinese). In: Institute of Geology, State Seismological Bureau, ed. Research on Modern Geodynamics and Its Application. Beijing: Seismological Press, 1994. 70–83
18 Wang T M, Li J P. The recurrence intervals of the strong earthquake in Tangshan (in Chinese). Seismol Geol, 1984, 6: 79–85
19 Ma J, Zhang B T, Yuan S R. Tangshan earthquake and the earthquake risk area (in Chinese). Seismol Geol, 1980, 2: 45–56
20 Qiang Z J, Zhang L R. Tangshan earthquake and Quaternary active faults. In: Committee on Seismogeology (in Chinese). The Seismological Society of China, ed. The Active Faults in China. Beijing: Seismological Press, 1982. 67–71
21 Gui K C, Geng S C. Worthwhile considering the seismo-structure of the Tangshan earthquake (in Chinese). Earthquake Res Chin, 1987, 3(Suppl.): 79–84
22 Li J H, Hao S J, Hu Y T, et al. A study on activity of the seismogenic fault for the Tangshan earthquake of 1976 (in Chinese). Seismol Geol, 1998, 20: 28–34
23 Hao S J, You H C. A detailed detection of the Tangshan active fault using shallow seismic survey (in Chinese). Seismol Geol, 2001, 23: 93–97
24 You H C, Xu X W, Wu J P, et al. Study on the relationship between shallow and deep structures in the 1976 Tangshan earthquake area (in Chinese). Seismol Geol, 2002, 24: 104–115
25 Qiu Z H, Ma J, Liu G X. Discovery of the great fault of the Tangshan earthquake (in Chinese). Seismol Geol, 2005, 27: 669–677
26 Jiang W L. Discussion on seismogenic fault of the 1976 Tangshan earthquake (in Chinese). Seismol Geol, 2006, 28: 312–318
27 Wu C. Investigation of earthquake disaster (in Chinese). In: Liu H X, ed. Disaster of Great Tangshan Earthquake (1). Beijing: Seismological Press, 1985. 203–209
28 Liu G D, Guo S M, Liu C Q. Background of Seismology and Geology (in Chinese). In: Editorial Group of "the 1976 Tangshan Earthquake", SSB. The 1976 Tanghan Earthquake. Beijing: Seismological Press, 1982. 71–130
29 Deng Q D, Wen X Z. A review on the research of active tectonics—History, progress and suggestions (in Chinese). Seismol Geol, 2008, 30: 1–30
30 Xu X W, Ji F J, Yu G H, et al. Reconstruction of paleoearthquake sequence using stratigraphic records from drill logs: A study at the Xiadian fault, Beijing (in Chinese). Seismol Geol, 2000, 22: 9–19
31 Jiang W L. Paleoearthquake analysis of the Xiadian fault since Late Period of Pleistocene Epoch from Pangezhuang boring in Beijing Plain (in Chinese). In: Department of Science and Technology, CEA, ed. Research on Active Fault (8). Beijing: Seismological Press, 2001. 140–148
32 Zhang S M, Wang D D, Liu X D, et al. Using borehole core analysis to reveal Late Quaternary paleoearthquakes along the Nankou-Sunhe Fault, Beijing. Sci China Ser D-Earth Sci, 2008, 51: 1154–1168
33 Yang X P, Zhang R Z, Zhang L F, et al. Some problems worth considering in the geological explanation of shallow seismic prospecting data (in Chinese). Seismol Geol, 2007, 29: 282–293
34 Lei Q Y, Chai C Z, Meng G K, et al. Composite drilling section exploration of Yinchuan buried fault (in Chinese). Seismol Geol, 2008, 30: 250–263
35 Matsuda T. Reading of paleoearthquake from stratum (in Japanese). Earth, 2000, 28(Suppl.): 10–15
36 Zhu Z C, Song H L. Structural Geology. Beijing: Publishing House of the University of Geological Science of China, 1990. 181–182
37 Chen W H, Ni M Y. Quaternary Geology of Hebei Provice (in Chinese). Beijing: Geological Publishing House, 1987. 1–186
38 Xie X S, Zhao J Q, Jiang W L, et al. Study on Holocene Paleoearthquake in Xizhang trench on the Jiaochen fault zone, Shanxi Province (in Chinese). Seismol Geol, 2007, 29: 744–755
39 Lin C Y, Chen X D, Shi L B. Microstructural and micro-sedimentologic analyses of the trench across the Jiaocheng fault, Xizhangcun village, Taiyuan, Shanxi Province (in Chinese). Seismol Geol, 2007, 29: 294–310
40 Jiang W L, Hou Z H, Xie X S. Research on paleoearthquakes in Jiuxian trenches across Nankou-Sunhe fault zone in Changping County of Beijing plain. Sci China Ser D-Earth Sci, 2002, 45: 160–173
41 Jiang W L, Hou Z H, Xiao Z M, et al. Study on Paleoearthquakes of Qixinzhuang trench at the Xiadian fault, Beijing plain (in Chinese). Seismol Geol, 2000, 22: 413–422